

# State of Health Estimation for Lithium-Ion Batteries

XiangRong Kong\* Arman Bonakdarpour\*\*  
Brian T. Wetton\* David P. Wilkinson\*\* Bhushan Gopaluni\*\*

\* *Department of Mathematics - University of British Columbia,  
Vancouver, BC V6T 1Z2, Canada*

\*\* *Department of Chemical and Biological Engineering - University of  
British Columbia, Vancouver, BC V6T 1Z3, Canada*

---

**Abstract:** The state of health (SoH) of lithium-ion batteries and battery packs must be monitored effectively for abuse to prevent failure and accidents, and to prolong the useful lifetime of the batteries. Many studies have suggested that temperature and discharge/charge current rate are the primary factors causing battery aging. However, there is yet to be a concrete mathematical model to predict the battery SoH. In this study, we introduce two SoH prediction models: the decreasing battery  $V_{0+}$  model, the increasing CV charge capacity model. Additionally, we derive a simple thermal model for the cell based on variation of temperature data.

*Keywords:* lithium-ion battery, state of health, temperature profile, state of charge

---

## 1. INTRODUCTION

Lithium-ion battery packs are a source for major or supplementary power for mobile applications such as electric vehicles, electric scooters, and also back-up power systems of several scales. A key aspect of the technology is their proprietary Battery Management Systems (BMS) that monitor the battery pack to maintain safe operation during charging and use, and allow some performance optimization. Such systems have a component that estimates the pack State of Charge (SoC), that is the amount of charge still in the pack to deliver application power. The simplest SoC indicators rely on an invariant model of the cell's performance to yield their output and do not take into account how a pack is changing over time. However, in reality the performance of batteries decreases over time and with use, described as a change in the battery's State of Health (SoH).

In recent years, a lot of attention has been focused on the diagnosis of lithium-ion battery SoH. Nearly all literature regard discharge/charge current rate and temperature as top factors affecting SoH. However, a concrete mathematical model which can connect these two factors to battery's SoH is still not available to authors' best knowledge.

In this study, batteries are discharged and charged over many cycles, while their voltage, capacity, current, and temperature profiles are recorded. Based on the data collected and analyzed, two models that can potentially predict battery SoH are presented.

## 2. EXPERIMENTAL

Cylindrical 18650 lithium-ion rechargeable cells (Panasonic NCR18650B, Figure 1) of Lithium Nickel Cobalt Aluminum Oxide ( $\text{LiNiCoAlO}_2$ ) chemistry are tested in

this work. The nominal cell voltage and capacity are 3.6V and 3.2Ah, respectively. The manufacturer recommended charge/discharge voltage boundaries are between 2.5 and 4.2V.



Fig. 1. Panasonic NCR18650B Lithium-ion Batteries

### 2.1 Galvanostatic cycling of single battery cells

Galvanostatic cycling is performed under room temperature within the manufacturer specified voltage range of 2.5-4.2V. Each cycle consists of six stages:

1. Constant current discharge at 1C, or 3.2A, until voltage reaches 2.5V
2. Open circuit voltage (OCV, 30 minutes)
3. Constant current charge at 1C until voltage reaches 4.2V
4. OCV (30 minutes)
5. Constant voltage charge at 4.2V for 4 hours
6. OCV (30 minutes)

A potentiostat (10A, VMP3 multi-channel potentiostat, BioLogic Science Instruments) was used to perform the discharge/charge cycles. Between each discharge/charge steps, the cell was relaxed for 30 minutes and the cell potential was recorded. Temperature of the cell during

cycling was recorded by self-adhesive (silicon based cement) K-type thermocouple temperature sensors (SA1-K-72, Omega Engineering Inc.) with better than 0.3 s response time. Two thermocouples were used: one attached to the main body of the cell and one attached to the anode tip of the cell. The cover of the cell was carefully removed where the self-adhesive thermocouple was attached. Temperature data were recorded by a high-speed 8-channel TCIC thermocouple interface card (TCIC-USB-ENC, Omega Engineering Inc.)

Figure 2 shows a typical current and voltage profile of the batteries for one discharge/charge cycle. During constant current discharging, the current is denoted as a negative value and the voltage decreases non-linearly until it reaches the cut-off voltage (2.5V). During constant current charge, the current is held constant with a rising voltage until the voltage reaches the maximum charging voltage (4.2V), at which point constant voltage charge begins.

In the experiment presented here, 101 cycles of battery current, voltage, and capacity are recorded. The first 31 cycles also have their temperature profile recorded.

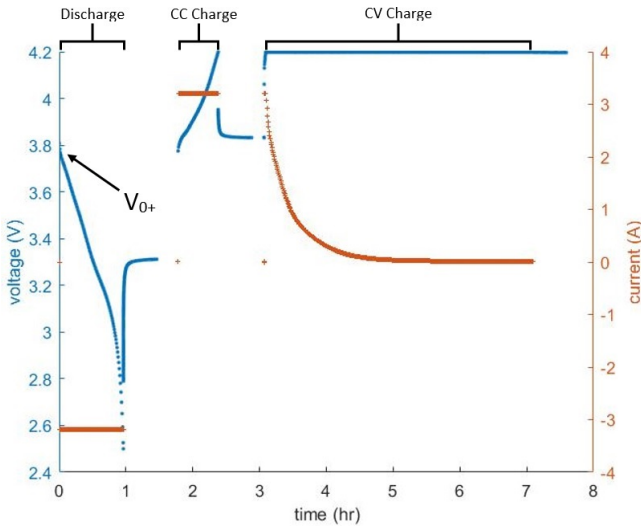


Fig. 2. Discharge/Charge Current and Voltage Profile

### 3. RESULTS AND DISCUSSION

#### 3.1 Voltage vs. Capacity Plots

Voltage vs. Capacity plots give crude estimation of battery degradation. As a battery is cycled, the charge decreases, indicating a loss of energy. Thus a leftward shift of voltage vs. capacity curves is expected.

Figure 3 shows voltage vs. capacity curves. Notice that both discharge and charge curves illustrate similar pattern: they move to the left over time, indicating that the capacity, or the amount of charge the battery is able to hold, decreases as it is cycled.

Figure 4 shows the battery temperature vs. time. Notice that there are relatively large room temperature fluctuations during the cycling processes.

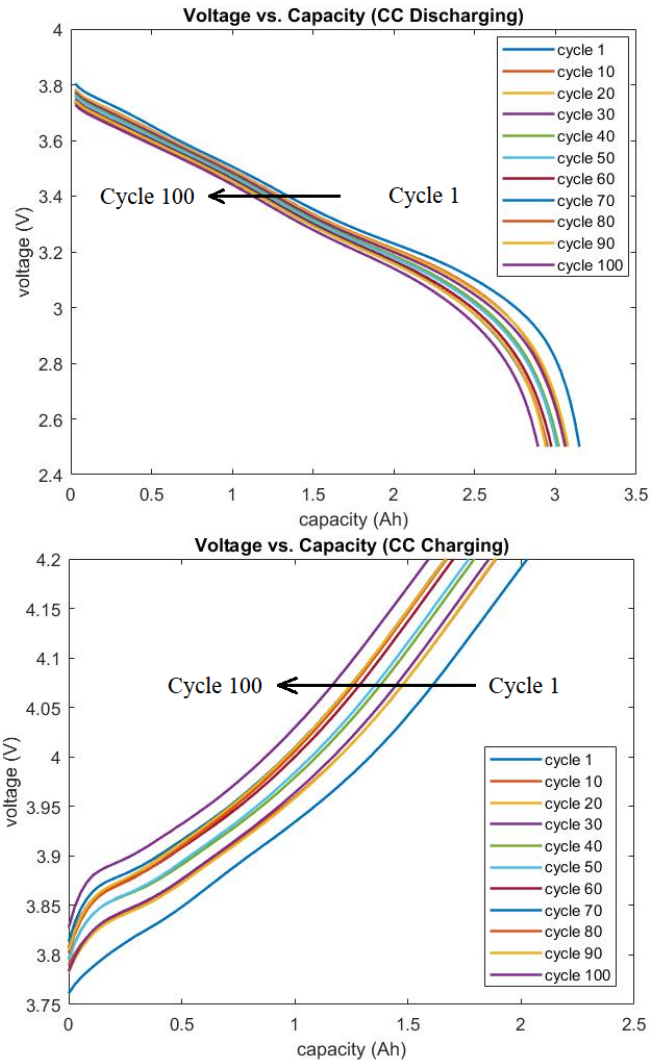


Fig. 3. Voltage vs. Capacity curves for a) constant current discharge and b) constant current charge

### 4. SOH PREDICTION MODEL

Present models of SoH prediction are based on large amounts of battery operation data. However, even the most sophisticated BMS has very limited data storage. Based on the assumption that voltage vs. capacity curves follow a similar pattern for varying discharge rates, the model presented in this section attempts to achieve the goal of SoH prediction through only a short history of battery operation, which makes BMS implementation highly feasible. Specifically, this model, given merely the voltage and percentage of charge drawn from the battery during discharging, attempts to predict the number of discharge/charge cycles the battery has performed through, a natural indicator of battery SoH.

#### 4.1 SoH prediction based on decreasing $V_{0+}$

Let  $\gamma$  denote the cycle number a battery has been discharged/charged through. Let  $V_{0+}$  be the voltage at the beginning of discharge (see Figure 2), with it a function of cycle number

$$V_{0+} = V_{0+}(\gamma) \quad (1)$$

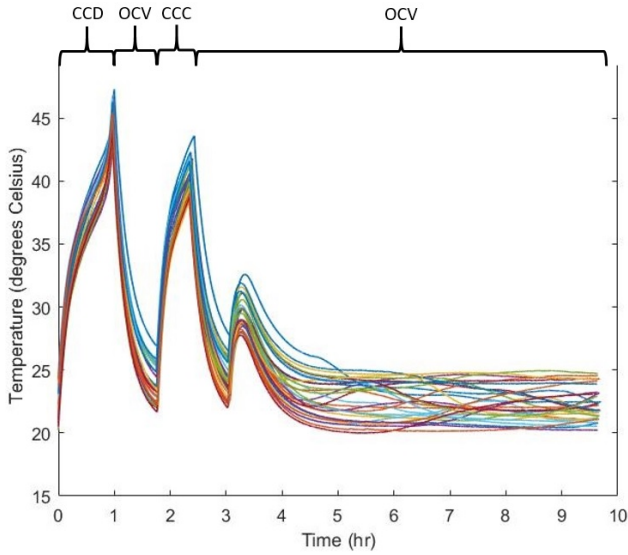


Fig. 4. Battery Temperature vs. Cycles

Recall that as the battery is cycled, the amount of charge it is able to hold decreases. Therefore, we expect  $V_{0+}$  to decrease as battery ages, shown in Figure 5. This property alone can be an indicator of battery SoH.

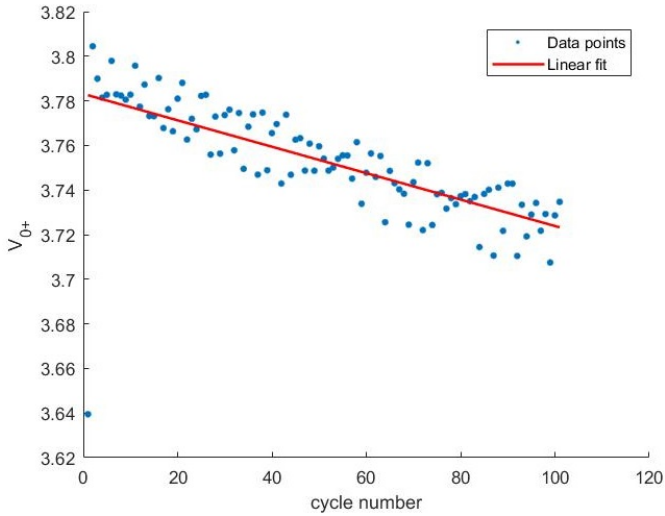


Fig. 5.  $V_{0+}$  vs. Cycle Number - with linear fit

Performing linear regression, we obtain the function

$$V_{0+}(\gamma) = \beta_0 + \beta_1\gamma \quad (2)$$

The linear fit superimposed on the data points as shown on the same figure. The values of  $\beta_0$  and  $\beta_1$  are listed in the table below

$\beta_0$	3.7831
$\beta_1$	-0.0006

Here,  $\beta_0$  represents the  $V_{0+}$  (V) of a new battery which has not gone through any discharge/charge cycles, while  $\beta_1$  represents the rate of  $V_{0+}$  decrease with respect to cycle number ( $\frac{V}{\gamma}$ ).

#### 4.2 SoH prediction based on increasing CV charging capacity

In real applications, constant current discharge/charge cannot be expected. For example, the driver of an electrical vehicle may accelerate for a few seconds, drawing a large current, followed by an immediate deceleration drawing a small current. However, the constant *voltage* charge (stage 5 in this study) is relatively much more consistent if it is run to completion, at the end of charging in an off duty period, for example. Therefore, measuring the change in capacity during constant voltage charge as a function of cycle number is another way to assess the SoH of the battery. This is shown in Figure 6.

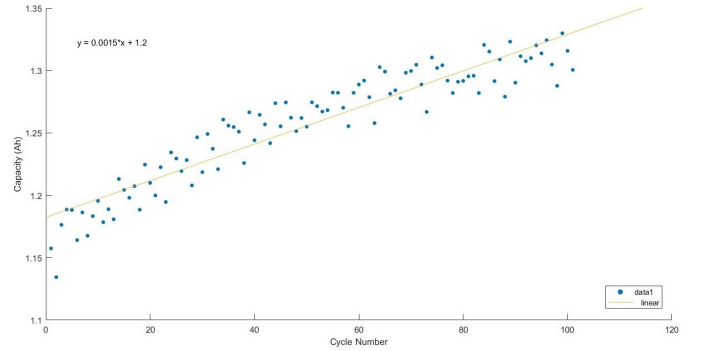


Fig. 6. Capacity vs. Cycle Number for constant voltage charge

Figure 6 shows that the capacity during constant voltage charge increases with cycle number, which is expected since as battery ages, the resistance increases and so the constant current charge reaches the cutoff voltage faster.

### 5. TEMPERATURE PROFILE MODELING

We now analyze the temperature profiles recorded and fit parameters to a simple thermal model.

#### 5.1 Temperature profile revisited

Figure 7 shows the close-up of the constant current discharge and OCV part of the temperature profile for each cycle. Here the rising temperature from 0 to 1 hour is caused by constant current discharge stage, whereas the temperature decrease to ambient from 1 to 1.8 hour represents the OCV stage. The linear trend in temperature has been removed to reduce the effect of room temperature variations.

The temperature profiles for all cycles are averaged and plotted in Figure 8. Decreasing of temperature in an exponential decay form suggests Newton's law of cooling, which can be modelled by

$$\frac{\partial T}{\partial t} = -k(T - T_{room}) \quad (3)$$

where  $k$  is a constant to be fitted.

The rising temperature, on the other hand, begins to show a plateau at approximately 0.6 hour (expected if the heat generation was constant in time), but experiences an inflection point and then increases sharply until constant

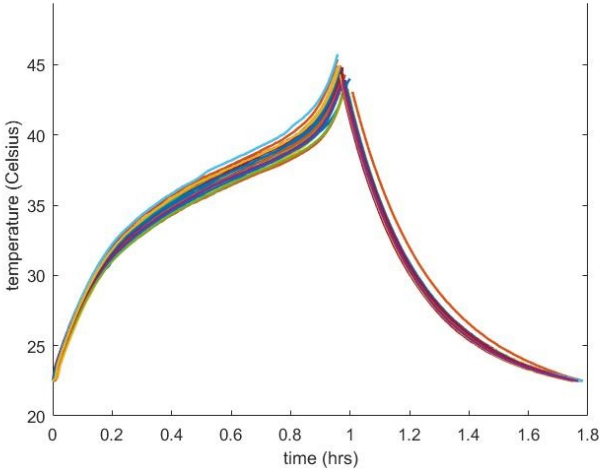


Fig. 7. Temperature (normalized) vs. Time for CCD and OCV

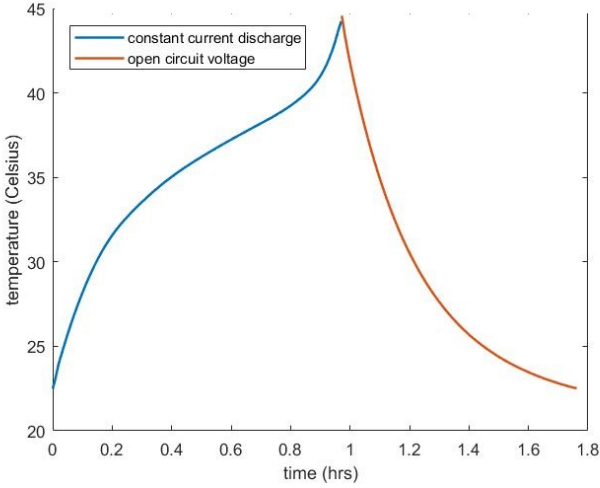


Fig. 8. Average Temperature (normalized) vs. Time for CCD and OCV

current charge is over at 1 hour. This suggests that there is an increasing volumetric heat generation term,  $g(t)$ , during discharge, as expected.

$$\frac{\partial T}{\partial t} = -k(T - T_{room}) + cg(t) \quad (4)$$

where  $k$  is the same constant as above, and  $c$  is another constant to be fitted. The inverse of  $c$  is the average thermal capacity of the cell.

According to Torchio *et al.*, this heat generation term originates from volumetric heating of the battery and has the form

$$g(t) = \frac{I(IR + \eta)}{\pi r^2 H} \quad (5)$$

where  $I$  is the current,  $R$  is the effective resistance,  $\eta$  is the overpotential, and  $r$  and  $h$  are radius and height of the cell, respectively. The denominator is the volume of the cell.

Decoupling the resistance from the overpotential is challenging from this set of data. We consider the average of the voltage difference from 1C charge and discharge in Figure 9. The difference, divided by 2, is relatively constant

in discharge capacity initially. Thus, we consider the initial  $(V_{cc} - V_d)/2I$  as the effective “resistance”  $R$ . Note that in Figure 9, the discharge capacity fraction begins at 0.4: as the cell charges, constant voltage charge begins when the cell voltage reaches 4.2V and the remaining charge percentage is added in a way that is not directly comparable to discharge.

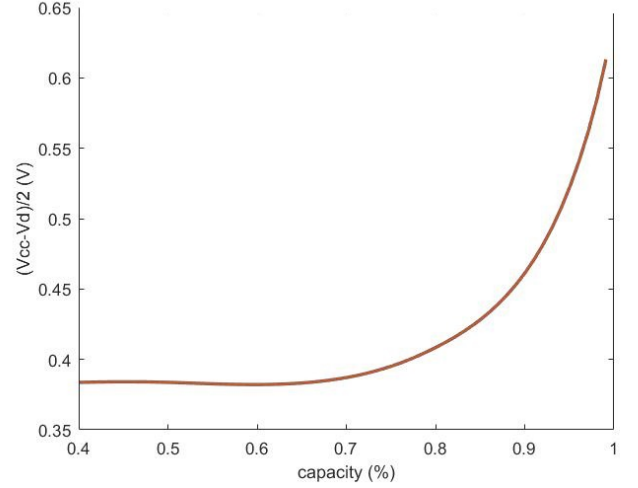


Fig. 9. Average  $(V_{cc} - V_d)/2$  vs. Normalized Capacity

Although there is an overpotential for both charge and discharge, we ascribe the overpotential  $\eta$  in equation 7 to predominantly the discharge, thus

$$IR + \eta = \begin{cases} (V_{cc} - V_d)_*/2 & \theta < \theta_* \\ V_{cc} - V_d - (V_{cc} - V_d)_*/2 & \theta > \theta_* \end{cases}$$

where  $\theta_*$  is the capacity at which constant current charge changes to constant voltage charge ( $\theta_* \approx 0.4$  as shown in Figure 9), and  $(V_{cc} - V_d)_*/2$  is the value of the voltage difference at this capacity (the left hand value on Figure 9)

## 5.2 Temperature fitting

The solution to equation (5) is

$$T(t) = T_i + (T_m - T_i)e^{k(t_m - t)} \quad (6)$$

And the solution to equation (6) is

$$T(t) = T_i + c \int_0^t g(s)e^{k(s-t)} ds \quad (7)$$

where  $t_i$  and  $T_i$  are the starting time and temperature of the rising temperature part, and  $t_m$  and  $T_m$  are the time and temperature of the decreasing temperature part.

By minimizing residuals to (8) and to numerical calculations of (9) to the experimental data, the values of  $k$  and the inverse of  $c$  are obtained as

$k$	4.4924
$1/c$	1000

The quality of the fit is shown in Figure 10.

By dimensional analysis,  $k$  has units of  $\frac{1}{s}$  and  $c$  has units of  $\frac{J}{m^3 k}$ . From the results,  $k$  is simply the constant of Newton’s law of cooling, while  $c$  is the inverse of average thermal capacity.

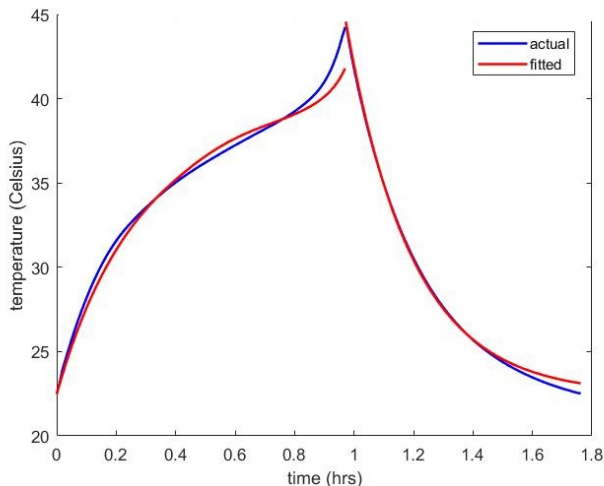


Fig. 10. Temperature Fitting for CCD and OCV

## 6. CONCLUSIONS

In this study, two models were proposed to predict Li-ion battery state-of-health (SoH): 1) the decreasing battery  $V_{0+}$  model and 2) the increasing CV charge capacity model. From the two models, battery aging is clear. Additionally, we derive a fitted thermal model that can be used to predict cell temperatures in other conditions. An interesting experiment currently in progress involves dividing the batteries into two batches: one batch is discharged/charged under different current rates under room temperature, whereas the other batch is thermocycled using the temperature profile generated from batch one but not discharged/charged. This experiment distinguishes battery aging due to cycling (discharge/charge) from purely temperature variation.

## REFERENCES

- Atebamba *et.al.*, On the Interpretation of Measured Impedance Spectra of Insertion Cathodes for Lithium-Ion Batteries *Journal of Electrochemical Society*, volume 157, pages 1218-28, 2010
- Dong *et.al.*, Lithium-ion Battery SOH Monitoring and Remaining Useful Life Prediction based on Support Vector Regression-Particle Filter *Journal of Power Sources*, volume 271, pages 114-123, 2014
- Fernandez *et.al.*, Capacity Fade and Aging Models for Electric Batteries and Optimal Charging Strategy for Electric Vehicles *Energy (Oxford)*, volume 60, pages 35-43, 2013
- Hausbrand *et.al.*, Fundamental Degradation Mechanisms of Layered Oxide Li-ion Battery Cathode Materials - Methodology, Insights and Novel Approaches *Material Science and Engineering*, volume 192, pages 3-25, 2014
- Love *et.al.*, State-of-Health Monitoring of 18650 4S Packs with a Single-Point Impedance Diagnostic *Journal of Power Sources*, volume 266, pages 512-9, 2014
- Omar *et.al.*, Lithium Iron Phosphate Based Battery - Assessment of the Aging Parameters and Development of Cycle Life Model *Applied Energy*, volume 113, pages 1575-85, 2013
- Salkind *et.al.*, Determination of State-of-Charge and State-of-Health of Batteries by Fuzzy Logic Methodology *Journal of Power Sources*, volume 80, pages 293-300, 1999
- Stroe *et.al.*, Diagnosis of Lithium-Ion Batteries State-of-Health based on Electrochemical Impedance Spectroscopy Technique *IEEE Energy Conversion Congress and Exposition*, pages 4576-82, 2014
- Torchio *et.al.*, LIONSIMBA: A Matlab Framework Based on a Finite Volume Model Suitable for Li-Ion Battery Design, Simulation, and Control *Journal of the Electrochemical Society*, pages 1192-1205, 2016
- Williart *et.al.*, Comparative Analysis of Features for Determining State of Health in Lithium-Ion Batteries *International Journal of Prognostics and Health Management*, volume 2(1), pages 14-20, 2013